

Research Paper

Traumatic spinal cord injury in mice with human immune systems



Randall S. Carpenter^{a,b,c}, Kristina A. Kigerl^{b,c}, Jessica M. Marbourg^{a,b,c}, Andrew D. Gaudet^{b,c}, Devra Huey^d, Stefan Niewiesk^d, Phillip G. Popovich^{a,b,c,*}

^a Neuroscience Graduate Studies Program, The Ohio State University, Columbus, OH, USA

^b Center for Brain and Spinal Cord Repair, The Ohio State University, Columbus, OH, USA

^c Department of Neuroscience, The Ohio State University, Columbus, OH, USA

^d Department of Veterinary Biosciences, The Ohio State University, Columbus, OH, USA

ARTICLE INFO

Article history:

Received 10 March 2015

Received in revised form 18 June 2015

Accepted 13 July 2015

Available online 17 July 2015

Keywords:

Spinal cord injury

Humanized mice

Inflammation

Neuroimmunology

Macrophages

Lymphocytes

Functional recovery

Stem cells

Hematopoiesis

ABSTRACT

Mouse models have provided key insight into the cellular and molecular control of human immune system function. However, recent data indicate that extrapolating the functional capabilities of the murine immune system into humans can be misleading. Since immune cells significantly affect neuron survival and axon growth and also are required to defend the body against infection, it is important to determine the pathophysiological significance of spinal cord injury (SCI)-induced changes in human immune system function. Research projects using monkeys or humans would be ideal; however, logistical and ethical barriers preclude detailed mechanistic studies in either species. Humanized mice, i.e., immunocompromised mice reconstituted with human immune cells, can help overcome these barriers and can be applied in various experimental conditions that are of interest to the SCI community. Specifically, newborn NOD-SCID-IL2rg^{null} (NSG) mice engrafted with human CD34⁺ hematopoietic stem cells develop normally without neurological impairment. In this report, new data show that when mice with human immune systems receive a clinically-relevant spinal contusion injury, spontaneous functional recovery is indistinguishable from that achieved after SCI using conventional inbred mouse strains. Moreover, using routine immunohistochemical and flow cytometry techniques, one can easily phenotype circulating human immune cells and document the composition and distribution of these cells in the injured spinal cord. Lesion pathology in humanized mice is typical of mouse contusion injuries, producing a centralized lesion epicenter that becomes occupied by phagocytic macrophages and lymphocytes and enclosed by a dense astrocytic scar. Specific human immune cell types, including three distinct subsets of human monocytes, were readily detected in the blood, spleen and liver. Future studies that aim to understand the functional consequences of manipulating the neuro-immune axis after SCI should consider using the humanized mouse model. Humanized mice represent a powerful tool for improving the translational value of pre-clinical SCI data.

© 2015 Elsevier Inc. All rights reserved.

1. Introduction

Mice are valuable experimental tools and are essential for understanding mechanisms of neural injury and repair. They are relatively inexpensive and are easy to use/manipulate. Moreover, their genome has been sequenced making genetic engineering strategies possible (Waterston et al., 2002). In addition, since the human genome also is known (Lander et al., 2001), spinal cord injury (SCI)-induced changes in the expression of mouse genes can be extrapolated to the human condition. However, recent data indicate that the composition and function of mouse and human immune systems are different (Mestas and Hughes, 2004), and therefore bridging scientific findings from mice to humans may be misleading. While human and mouse transcriptional

profiles of immune cells are relatively conserved, hundreds of genes display extensive divergence (Shay et al., 2013). Further, genomic responses in mouse models of inflammation do not always match what is observed in the associated human condition (Seok et al., 2013). While this does not negate the utility of current mouse models, it does suggest caution when bridging discoveries across the species barrier from mice to humans.

In recent years humanized mice have been developed to model specific human diseases (e.g., HIV infection) that cannot be studied in traditional mouse strains. “Humanized mice” refer to immature immunodeficient mice that are injected with human blood stem cells. As they mature, these mice develop a functional human immune system (Shultz et al., 2007, 2012). While many models and background strains have been used for this purpose, the NOD-SCID-IL2rg^{null} (NSG) mouse is particularly effective at engrafting human blood stem cells and developing a wide range of functional human immune cell lineages (Coughlan et al., 2012; Brehm et al., 2010; Giassi et al., 2008; Ishikawa et al., 2005; Rajesh et al., 2010; Shultz et al., 2005; Tanaka et al., 2012).

* Corresponding author at: Center for Brain and Spinal Cord Repair, The Ohio State University, 694 Biomedical Research Tower, 460 W. 12th Ave., Columbus, OH 43210, USA. E-mail address: phillip.popovich@osumc.edu (P.G. Popovich).

The goal of the current study was to characterize the anatomical, functional and hematological consequences of a standardized contusive spinal cord injury (SCI) in humanized NSG (hNSG) mice. The data indicate that in all cases, humanized mice respond like other mouse strains to experimental traumatic SCI. Here, we establish that the humanized mouse model is an unrealized but potentially powerful tool for understanding human neuroimmune biology and systemic immune function in the context of dynamic protracted neurological diseases including SCI.

2. Methods

2.1. Development and care of humanized NSG mice

The Institutional Animal Care and Use Committee of The Ohio State University approved all animal protocols. Young adult breeding pairs of NOD.Cg-Prkdc^{scid} Il2rg^{tm1Wjl}/SzJ mice (NSG mice) were purchased from The Jackson Laboratory (Bar Harbor, ME). Animals were fed commercial food pellets and chlorinated reverse osmosis water ad libitum, and housed in ventilated microisolator cages layered with corn cob bedding in a 12 hour light–dark cycle at a constant temperature ($20 \pm 2^\circ\text{C}$) and humidity ($50 \pm 20\%$). In total, 5 male and 6 female newborn NSG mice were selected for hematopoietic stem cell engraftment procedures. Newborn NSG pups (24–48 h postnatal) received 100 cGy whole body irradiation (RS 2000, Rad Source, Suwanee, GA). Human umbilical cord CD34⁺ stem cells (Lonza Incorporated, Walkersville, MD) were thawed according to the manufacturer recommended protocol then were suspended in Hematopoietic Growth Media (Lonza Inc.) supplemented with StemSpan CC100 (Stemcell Technologies, Vancouver, BC). Immediately after irradiation, each mouse was lightly anesthetized on ice and subjected to a single intrahepatic injection of $3\text{--}5 \times 10^4$ cells in a total volume of 50 μl into the right lateral lobe using a sterile 26 gauge needle. After the procedure body temperature was maintained at 37°C using a heating pad. Once recovered, newborn NSG mice were returned to their dams for normal maturation until weaning at 21 days. At that time they were housed ≤ 5 mice per cage for the duration of the experiment. All mice survived irradiation and engraftment procedures. Engraftment of human peripheral blood leukocytes was initially assessed 10 weeks after injection (see flow cytometry methods below).

2.2. Spinal cord contusion injury

Thirteen weeks after engraftment, hNSG mice ($n = 11$) were subjected to a moderate mid-thoracic (T9) spinal cord contusion injury. Non-irradiated, non-engrafted NSG mice served as controls ($n = 8$ mice; $n = 4$ male and $n = 4$ female). Mice were anesthetized with a ketamine/xylazine cocktail (120 and 10 mg/kg intraperitoneal, respectively), hair was shaved at the region of the thoracic spinal cord, and skin treated with a sequence of betadine, 70% ethanol, and betadine. A small midline incision was made to expose the T9 vertebra then a partial laminectomy was performed followed by a 60 kdyn contusion injury using an Infinite Horizon Impactor (Precision Systems and Instrumentation, Lexington, Kentucky). Force and displacement biomechanics were measured for each injury. Body temperature was maintained at 37°C during surgery using a heat pad. After SCI, skin was closed using sterile wound clips then mice were returned to their cages which were placed overnight onto a slide warmer set to 37°C . Sterile saline (2 ml) was injected subcutaneously after SCI to maintain proper hydration. Bladders were manually expressed twice daily for the duration of the study. Gentocin antibiotic was subcutaneously administered once a day at 5 mg/kg for 5 days after injury. One female hNSG mouse died immediately prior to SCI surgery, likely due to complications from anesthesia, and one male hNSG mouse died during the post-injury period. Both mice were excluded from all analyses. hNSG and NSG mice were not injured on the same days. However, all animals were subjected to nearly identical injury force and displacement: 61.9 ± 0.5 kdyn and displacement of 497 ± 5 μm for

hNSG mice and 62.0 ± 0.6 kdyn and displacement of 475 ± 19.5 μm for NSG mice.

2.3. Behavioral testing

Hindlimb motor function was assessed using the Basso Mouse Scale (Basso et al., 2006). Testing occurred 1 day prior to injury then again at 1, 3, 7, 14, 21, and 28 days post-injury (dpi). hNSG mice were placed into an open field and allowed to freely explore the environment for 4 min. The same two individuals scored hindlimb locomotor parameters during each test period. Left and right hindlimb BMS scores were averaged for each mouse to obtain a single value at each time point.

2.4. Flow cytometry

Assessment of human peripheral blood leukocytes (PBLs) was initially performed 10 weeks after engraftment with human umbilical stem cells. Approximately 50 μl whole blood was collected from the facial vein into a tube containing ethylenediaminetetraacetic acid (EDTA). Red blood cells were lysed with BD Pharm Lyse™ Lysing Buffer (BD Biosciences, Franklin Lakes, New Jersey). Antibodies against human leukocyte markers were added to aliquots of blood and allowed to incubate for 30 min at room temperature. A FACS Calibur flow cytometer (BD Biosciences) was used to analyze blood samples. Forward scatter and side scatter parameters were used to gate viable cell populations for further phenotypic analyses using antibody panels described in (Table 1). Offline data analyses were completed with FlowJo v.10 software (Tree Star, Inc., Ashland, OR).

2.5. Tissue procurement and histology

At 28 dpi, hNSG mice were anesthetized and transcardially perfused with 0.1 M phosphate buffer saline (PBS) followed by 4% paraformaldehyde (PFA) in PBS. Tissues were post-fixed in 4% PFA for 2 h, dialyzed in 0.2 M phosphate buffer overnight at 4°C then cryopreserved in a 30% sucrose solution for 72 h at 4°C . Tissues were embedded in OCT medium (Sakura Finetek, Torrance, CA), frozen on dry ice, sectioned at 10 μm on a cryostat then stored at -20°C . For peroxidase and fluorescent based staining procedures slides were thawed at room temperature for 1 h, placed on a slide warmer for 1 h and then rinsed in 0.1 M PBS.

For immunohistochemistry, sections were overlaid with 4% BSA and 0.1% Triton X-100 in 0.1 M PBS for 1 h followed by primary antibody overnight at 4°C . After PBS washes ($3 \times$), sections were incubated with secondary antibodies at room temperature for 1 h. Immunoperoxidase labeling required quenching of endogenous peroxidases with 6% H_2O_2 diluted in methanol for 15 min at room temperature prior to incubation with Vectastain ABC (Vector Laboratories, Burlingame, CA) for 1 h at room temperature. Bound antibody was visualized by overlaying sections with 3,3'-diaminobenzidine (DAB, Vector Laboratories) for 5–15 min (until optimal differentiation of signal). To reduce non-specific labeling caused by using mouse primary antibodies on mouse tissues, primary and secondary antibodies were mixed at 37°C for 1 h then normal mouse serum was added for an additional hour at 37°C at a dilution of 1:1000. The antibody mixture was allowed to cool on ice for 1–2 h. The primary and secondary antibody complex was overlaid onto tissue sections overnight at 4°C , followed by ABC amplification and DAB development as described above.

A separate protocol was used to identify human immune cell types. After thawing, tissue sections were placed in ice-cold methanol for 20–30 min, followed by washes in PBS. When required (i.e. hCD3), antigen retrieval was accomplished by incubating tissues in heated alkaline pH Tris-based solution (H-3301, Vector Laboratories) followed by a blocking step using a mixture of 4% BSA, 3% normal goat serum and 0.1% Triton X-100 in 0.1 M PBS for 1 h. Sections were incubated with primary antibodies overnight at 4°C , followed by washes in PBS

Table 1
Antibodies used for flow cytometry and immunohistochemical staining.

Marker	Host species	Clone	Vendor	Cat #	Volume/dilution	Conjugate
Human CD45 (LCA)	Mouse	2D1	BD Biosciences	347464	10–20 μ l per test ^a	PerCP
Human CD16 (Fc γ RIII)	Mouse	3G8	BD Biosciences	555406	10–20 μ l per test ^a	FITC
Human CD14	Mouse	MOP9	BD Biosciences	562691	10–20 μ l per test ^a	PE
Human CD3	Rat	CD3-12	Serotec	MCA1477	1:100–1:1000	
Mouse CD45	Rat	30-F11	BD Biosciences	553078	1:200	
CD45R/B220	Rat	RA3-6B2	Serotec	MCA1258G	1:200	
CD31 (PECAM-1)	Rat	MEC 13.3	BD Biosciences	553370	1:2000	
Collagen IV	Rabbit	–	Millipore	AB756	1:1000	
GFAP	Rabbit	–	Dako	Z0334	1:400	
Iba-1	Rabbit	–	Wako	019-19741	1:250–1:1500	
Laminin	Rabbit	–	Sigma	L9393	1:500	
NFH	Chicken	–	Aves	NF-H	1:1000	
<i>Isotype controls</i>						
IgG1 PE Isotype	Mouse	X40	BD Biosciences	340762	10–20 μ l per test ^a	PerCP
IgG1 FITC Isotype	Mouse	X40	BD Biosciences	340755	10–20 μ l per test ^a	FITC
IgG2b PE Isotype	Mouse	MPC-11	BD Biosciences	559529	10–20 μ l per test ^a	PE

^a Denotes volume used per peripheral blood sample for flow cytometry. All other dilutions used for immunohistochemical and immunofluorescent staining.

and subsequent incubation at room temperature for 1 h with Alexa Fluor-conjugated secondary antibodies. Nuclei were counterstained with DAPI. Information regarding antibody sources, working concentrations, and specificity are reported in Table 1.

Photomicrographs of immunolabeled tissue were captured using an AxioPlan 2 imaging microscope equipped with an AxioCam digital camera and AxioVision v.4.8.2 software (Carl Zeiss Microscopy GmbH, Jena, Germany). An Olympus FV1000 spectral confocal microscope with 20 \times and 60 \times oil objectives (Olympus America Inc., Melville, NY) was used to capture single plane images, maximum intensity projections of confocal Z stacks or orthogonal views for co-localization of fluorescent labeling when appropriate. Image stacks were saved as Olympus OIB files and digital images as 24 bit color TIFF files.

2.6. Data analysis

Data were analyzed using GraphPad Prism software (version 5.0, La Jolla, CA), and statistical significance was assigned to a $p < 0.05$. Except where noted, data are represented as mean \pm standard error of the mean. All figures were generated in Adobe Photoshop CS5 v.12 (Adobe Systems Inc., San Jose, CA).

3. Results

3.1. Analysis of human CD34⁺ stem cell engraftment before and after SCI in hNSG mice

First, the percentage of live peripheral blood leukocytes (PBLs) that express human leukocyte common antigen (hCD45) was quantified in uninjured NSG mice beginning 10 weeks after intrahepatic injection of human CD34⁺ umbilical cord stem cells. Identical analyses were completed in the same mice at 4 weeks post-SCI. At both times, blood samples were collected then analyzed using three-color flow cytometry. Live cells were gated from forward and side-scatter plots then the relative expression of hCD45 was measured. hCD45 is a high molecular weight transmembrane protein that distinguishes human blood leukocytes from residual mouse leukocytes. Consistent with previous reports (Lepus et al., 2009; Tanaka et al., 2012), ~8% of PBLs were hCD45⁺ 10 weeks after engraftment (Fig. 1A–D). When assessed 4 weeks post-SCI (17 weeks post-injection of hCD34⁺ cells), 57% of PBLs were hCD45⁺ ($p < 0.0001$, unpaired t-test, 17 vs. 10 weeks) (Fig. 1D). These data indicate efficient engraftment of human immune cells in NSG mice and a possible increase in hematopoiesis after SCI. Indeed, a 7-fold increase in human PBLs in hNSG mice after SCI is consistent with the post-SCI leukocytosis that develops in human SCI (Furlan et al., 2006; Riegger et al., 2009); however, to unequivocally prove an increase

in post-injury hematopoiesis, a more detailed time-course analysis of human immune cell reconstitution, with and without SCI, is required.

Monocytes are circulating precursors for tissue macrophages that dominate sites of inflammation. After SCI, whether monocyte-derived macrophages cause injury or repair is determined by their phenotype and activation state (Kigerl et al., 2009). In humans, there are three functionally distinct monocyte subpopulations; CD14hi/CD16neg (“classical”), CD14low/CD16low (“intermediate”) and CD14low/CD16hi (“non-classical”) (Auffray et al., 2009; Cros et al., 2010). Importantly, changes in the ratio of these monocyte subsets have clinical implications and could predict tissue injury as has been described in stroke (Urra et al., 2009). Here, we confirmed that in the blood of hNSG mice after SCI, ~25% of human PBLs were monocytes. This is consistent with the proportion of circulating monocytes described by other laboratories using hNSG mice (Rongvaux et al., 2014). Moreover, all relevant human monocyte subpopulations exist after SCI in hNSG mice (Fig. 1A–C,E). Limited blood samples and reagents precluded us from completing a detailed phenotypic analysis of other leukocyte subpopulations; however, based on size and relative expression of CD16, other CD14neg/CD16⁺ cell populations are likely human neutrophils and/or natural killer cells (Lanier et al., 1986; Huizinga et al., 1990).

3.2. Human immune cells populate peripheral lymphoid organs

After SCI, the liver and spleen play important roles in initiating systemic inflammation (Anthony and Couch, 2014; Blomster et al., 2013). For example, hepatocytes produce cytokines and chemokines that influence the activation and recruitment of monocytes to the CNS (Campbell et al., 2005, 2008). After SCI, leukocytes are recruited to the liver where they contribute to liver dysfunction (Fleming et al., 2012; Sauerbeck et al., 2015). The liver and spleen also are reservoirs for immune cells, including macrophages, T and B cells, and hematopoietic progenitors. In mice and humans, determining the dynamics of changes in immune cell function and hematopoiesis within these extramedullary reservoirs may be key for understanding a range of immune-related phenomena that occur after SCI (e.g., protracted/non-resolving intraspinal inflammation, systemic autoimmunity, chronic immunosuppression) (Schwab et al., 2014).

In hNSG mice, human immune cells were detected in the liver and spleen in anatomically appropriate locations (Fig. 2A,B). In the spleen, a full complement of innate and adaptive immune cells was identified including human macrophages (hCD45⁺/Iba-1⁺), T lymphocytes (hCD45⁺/hCD3⁺) and B lymphocytes (hCD45⁺/B220⁺) (Fig. 2C–E). Human T and B cells were primarily localized to splenic white pulp, while human macrophages were distributed throughout adjacent red

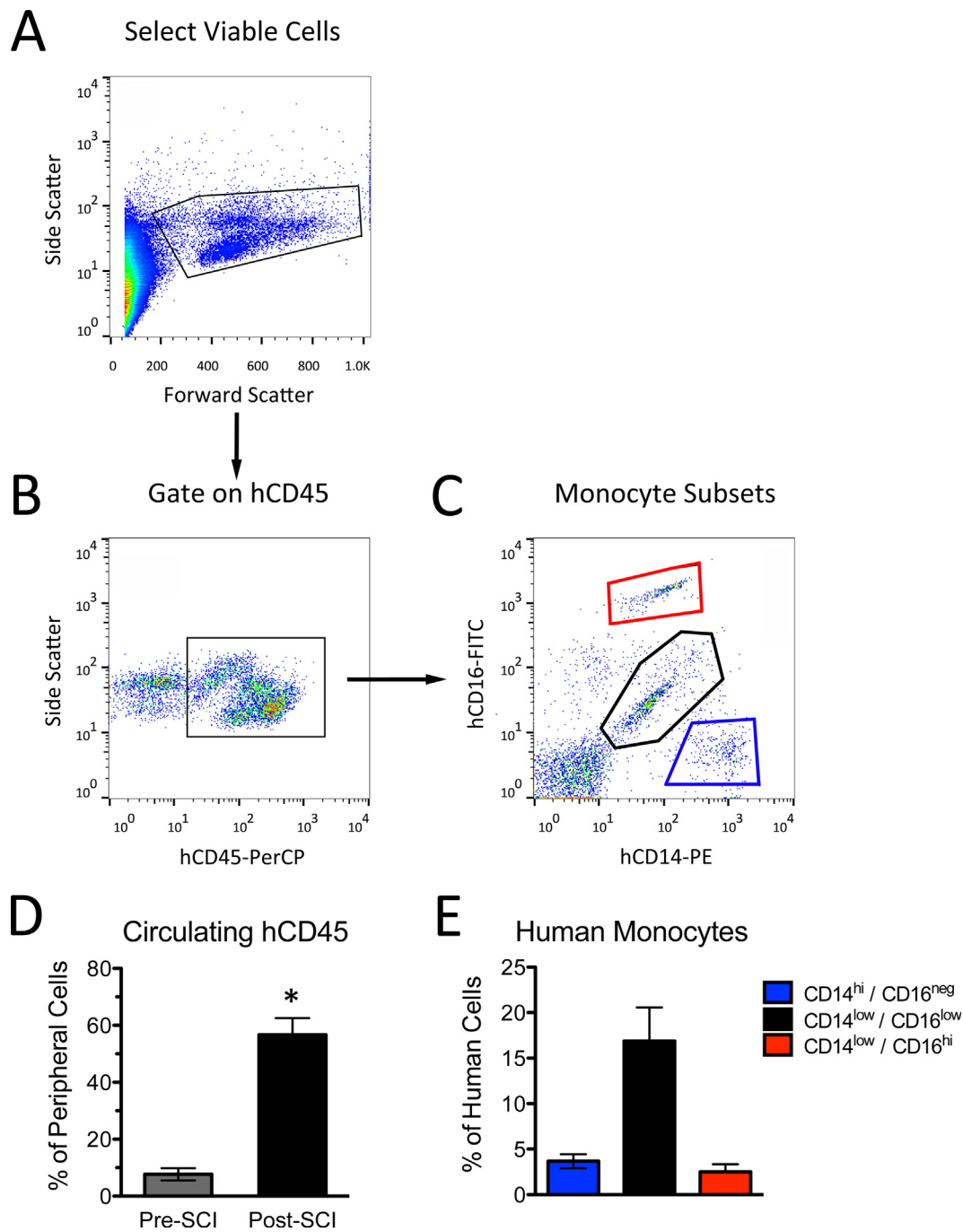


Fig. 1. Flow cytometry scatter plots illustrate the gating strategy used to detect human immune cells in peripheral blood of hNSG mice. The example shown in Fig. 1A–C is from a SCI hNSG mouse at 28 dpi. (A) Size (forward scatter) and granularity (side scatter) of peripheral blood leukocytes (PBLs) were used to select viable cells for phenotypic analysis. (B) From the viable cell population, the percentage of cells in hNSG mice expressing human CD45 (hCD45) was determined. (C) After gating on hCD45, relative expression levels of human CD14 (hCD14) and human CD16 (hCD16) were used to quantify monocyte subsets (red, black, and blue gates). (D) The percentage of human immune cells in the periphery of hNSG mice increased after SCI (* $p < 0.01$ vs. pre-SCI). (E) After SCI, monocytes represented ~25% of human PBLs, consisting mostly of CD14^{low}/CD16^{low} intermediate monocytes. (For interpretation of the references to color in this figure legend, the reader is referred to the web version of this article.)

pulp. In the liver, human leukocytes (hCD45⁺) surrounded liver sinusoids (Fig. 2B).

3.3. Spontaneous functional recovery and lesion histopathology after SCI in humanized mice are indistinguishable from that in other immune competent mouse strains

Both genetics and injury severity affect the overall magnitude of spontaneous locomotor recovery after SCI; however, the time course and patterns of recovery are nearly identical across all mouse strains

(Basso et al., 2006). To determine if recovery from SCI is unique in hNSG mice or control immunodeficient NSG mice, mice of both strains received moderate spinal contusion injuries then spontaneous recovery of locomotor function was analyzed. Since differences between mouse strains have been described previously (Basso et al., 2006), we focus here on changes specific to hNSG and NSG mice. Historical pre- and post-SCI data for other mouse strains (BALB/c and C57BL/6) are shown for reference.

Before SCI, open field locomotor function, as defined by the Basso Mouse Scale, was identical in all NSG and hNSG mice (BMS score and

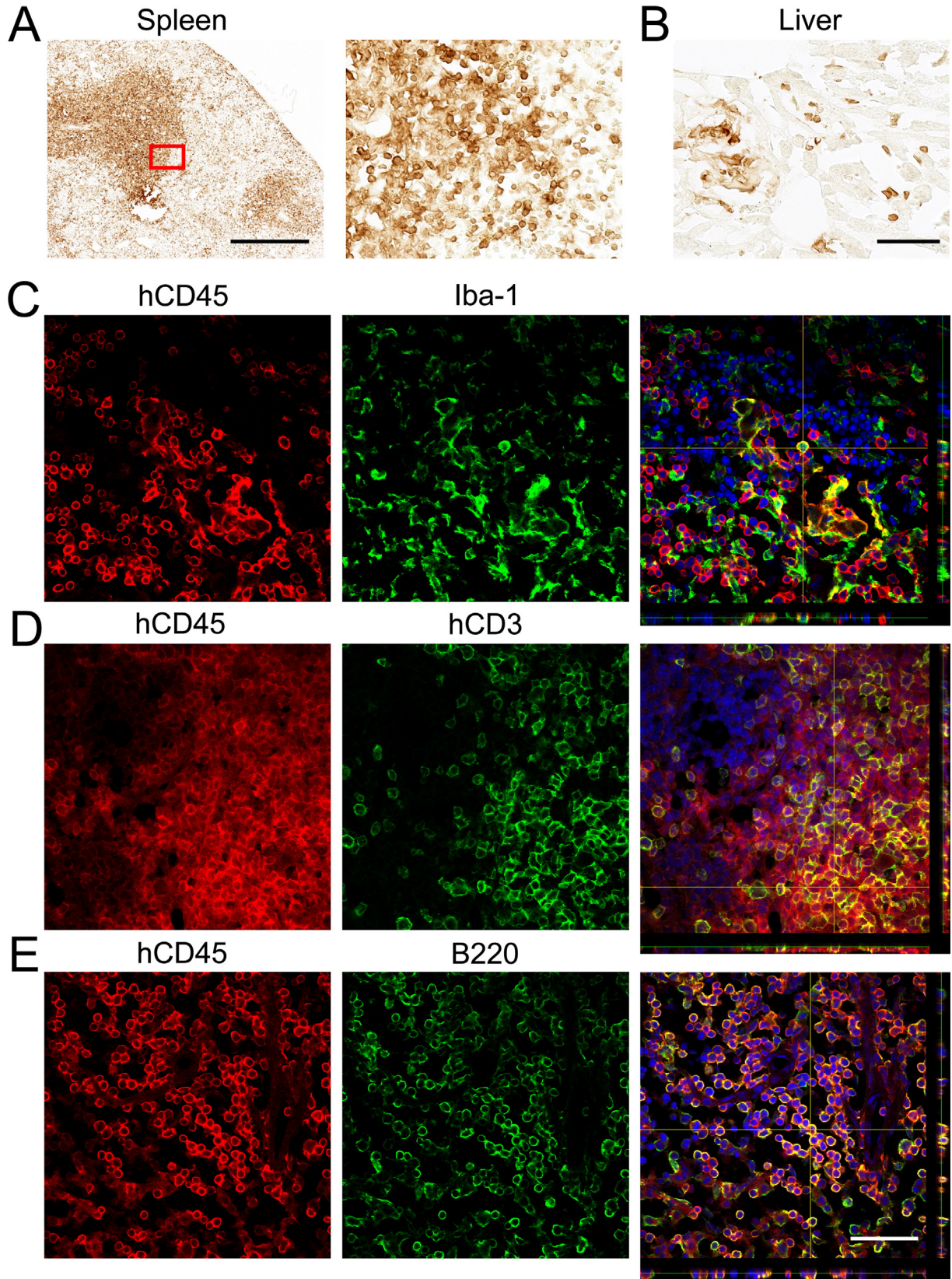


Fig. 2. Immunolabeling of hCD45 in peripheral organs 28 days post-injury (dpi) reveals human immune cells in the spleen (A) and liver (B) of hNSG mice. Although distributed throughout the spleen, human immune cells were most dense in cell clusters reminiscent of white pulp. (C) Human macrophages (hCD45⁺/Iba-1⁺), T lymphocytes (hCD45⁺/hCD3⁺), and B lymphocytes (hCD45⁺/B220⁺) were identified in the spleen of hNSG mice by confocal microscopy. Single plane (individual channels) and orthogonal views (combined channels) are shown, confirming co-localization of immunofluorescence. Blue = DAPI nuclear stain. Scale bar in A = 500 μ m, B = 50 μ m, and E = 50 μ m. (For interpretation of the references to color in this figure legend, the reader is referred to the web version of this article.)

subscores = 9 and 11, respectively) (Fig. 3A,B). After SCI, the onset of paralysis and rates of spontaneous functional recovery were nearly identical in hNSG and NSG mice (Fig. 3A). However, overall recovery was improved in immunodeficient NSG mice as compared with hNSG mice (Fig. 3A). By 14 dpi, 100% of NSG mice ($n = 5/5$ mice) recovered frequent or consistent plantar stepping with one mouse achieving coordination (BMS ≥ 5). Conversely, 55% of humanized mice ($n = 5/9$) achieved frequent or consistent plantar stepping by 14 dpi and none achieved coordinated locomotion (χ^2 of NSG and hNSG, $p = 0.078$).

After 14 dpi, general patterns of locomotor recovery plateau in all mouse strains; however, BMS subscore analyses reveal that other aspects of locomotion (e.g. frequency of plantar stepping, paw position, and trunk stability) continue to improve and strain-dependent differences exist (Fig. 3B). Specifically, while all NSG mice achieve BMS subscores ≥ 1 by 14 dpi, this occurred in only 4/9 hNSG mice ($p < 0.05$, χ^2).

Although recovery of hindlimb function in hNSG mice is worse than NSG mice, hNSG mice are on par with mouse strains with functional murine immune systems. The better functional recovery in immunodeficient NSG mice is consistent with other reports that have documented improved functional recovery after SCI in other strains of immunocompromised rats and mice (Luchetti et al., 2010; Potas et al., 2006).

Spinal cord histopathology in NSG and hNSG mice is comparable to that of other mouse strains (Inman et al., 2002; Kigerl et al., 2006; Sroga et al., 2003). By 28 dpi at the lesion epicenter, gray matter and a large portion of white matter are replaced by a fibrotic tissue mass and the lesion expands both rostral and caudal to the epicenter into dorsal column white matter. A major distinction, however, was that significantly less tissue (axons and myelin) was spared at the lesion epicenter in hNSG mice as compared with NSG control mice (26% vs. 48%; $p < 0.01$; Fig. 3C,E,F). The average lesion volume in SCI hNSG mice was identical to that of C57BL/6 and BALB/c mice after SCI but was

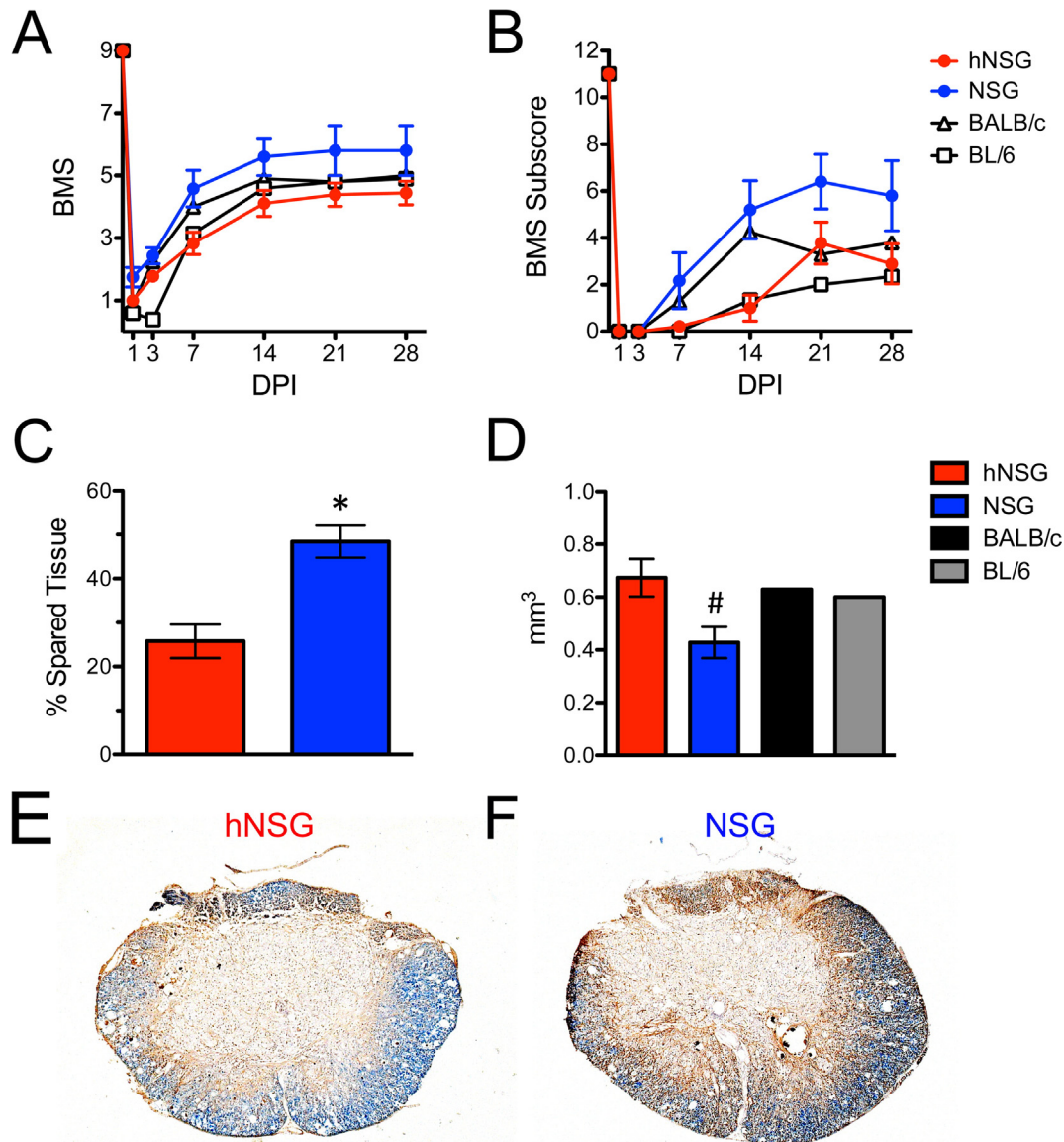


Fig. 3. Humanized mice develop severe functional impairment and lesion pathology after SCI that are reminiscent of other mouse strains; however, both outcome parameters are exacerbated in humanized mice (hNSG) as compared with immunodeficient NSG mice. (A&B) Hindlimb motor function was assessed using the Basso Mouse Scale (BMS) and BMS subscore. BMS score ($p = 0.054$) and subscore ($p < 0.05$) were better in NSG mice vs. hNSG mice; repeated measure 2-way ANOVA. (C) Significantly greater tissue sparing was evident in NSG mice as compared with hNSG mice ($26\% \pm 4$ vs. $48\% \pm 4$ respectively; $p < 0.01$; t-test). (D) Lesion volume in hNSG mice was identical to other mouse strains, but was significantly larger than NSG mice (0.67 ± 0.07 mm³ vs. 0.43 ± 0.06 mm³; $\#p < 0.05$, t-test). (E,F) EC/NFH stained epicenter sections from injured mice with tissue sparing closest to the group mean (i.e., ~27% for hNSG and 44% for NSG). Historical BMS and lesion volume data from BALB/c and BL/6 mice are provided for reference and are reprinted with permission.

significantly larger than lesions found in immunodeficient NSG mice (0.67 mm^3 vs. 0.43 mm^3 ; $p < 0.05$; Fig. 3D).

These data indicate that patterns of functional recovery and associated histopathology in SCI hNSG mice are stereotypical but are impaired or exacerbated relative to genetically identical mice that lack a functional immune system. Ongoing studies will attempt to define the functional implications of human immune cells recruited to the injury site. The remainder of this manuscript will focus on characterizing baseline cellular responses to SCI in hNSG mice.

3.4. Intraspinal inflammation in humanized mice

At the epicenter, the lesion core is surrounded by a rim of “spared white matter” containing neurofilament-positive axons (Figs. 3E,F and 4A). Surrounding the lesion is a dense astrogliotic (GFAP⁺) scar (Fig. 4B; arrowheads). Large and small hCD45⁺ human leukocytes infiltrate the injured spinal cord, primarily within the core of the lesion epicenter (Fig. 4C,D).

Large round, presumably phagocytic, hCD45⁺/Iba1⁺ macrophages dominate the lesion epicenter and lesion borders (Fig. 5A). Smaller and morphologically distinct hCD45⁺ cells also were found within the lesion epicenter. Immunofluorescent double-labeling and confocal imaging confirmed that these smaller cells are human T (hCD45⁺/hCD3⁺) and B lymphocytes (hCD45⁺/B220⁺) (Fig. 5B,C). Human T cells were found in clusters, interspersed among phagocytic human macrophages. However, some T cells were identified just outside the lesion core. hCD45⁺/B220⁺ B cells also infiltrated the injured hNSG spinal

cord. Consistent with observations in injured human spinal cords (Fleming et al., 2006), B cells within the lesion were sparse and were only found in a small subset of hNSG mice.

In hNSG mice, some host (mouse) immune cells persist, most notably myeloid cells (e.g., neutrophils, microglia and macrophages). To provide a qualitative overview of differences in the magnitude of resident and recruited human immune cells at 28 dpi and their relative distribution throughout lesioned/spared tissues, sections cut from the lesion epicenter and regions distal to the epicenter were double-labeled with hCD45 and mouse CD45 antibodies (Fig. 6). Within the lesion core, hCD45⁺ cells predominate; few resident mCD45⁺ cells were observed in the same sections (Fig. 6A–C). This spatial distribution is consistent with previous data obtained from mouse and rat bone marrow chimeras in which most cells within the lesion core are derived from the circulation; i.e., they are infiltrating leukocytes (Blomster et al., 2013; Popovich and Hickey, 2001; Mawhinney et al., 2012; Shechter et al., 2009). This conclusion is further supported by the fact that hCD45⁺ staining was absent in sections caudal to the injury epicenter or in tissue regions devoid of frank pathology (Fig. 6D,E). These latter regions are dominated by phagocytic or stellate mCD45⁺ cells resembling microglia.

Data above indicate that a complex human inflammatory reaction occupies the lesion epicenter of SCI humanized mice. Defining the functional significance of the infiltrating human immune cells will require additional research; however, if the presence of a xenogeneic inflammatory response adversely affects indices of endogenous CNS repair, it would obviate data interpretation for future intervention studies and minimize the utility of the current model. Accordingly, we analyzed

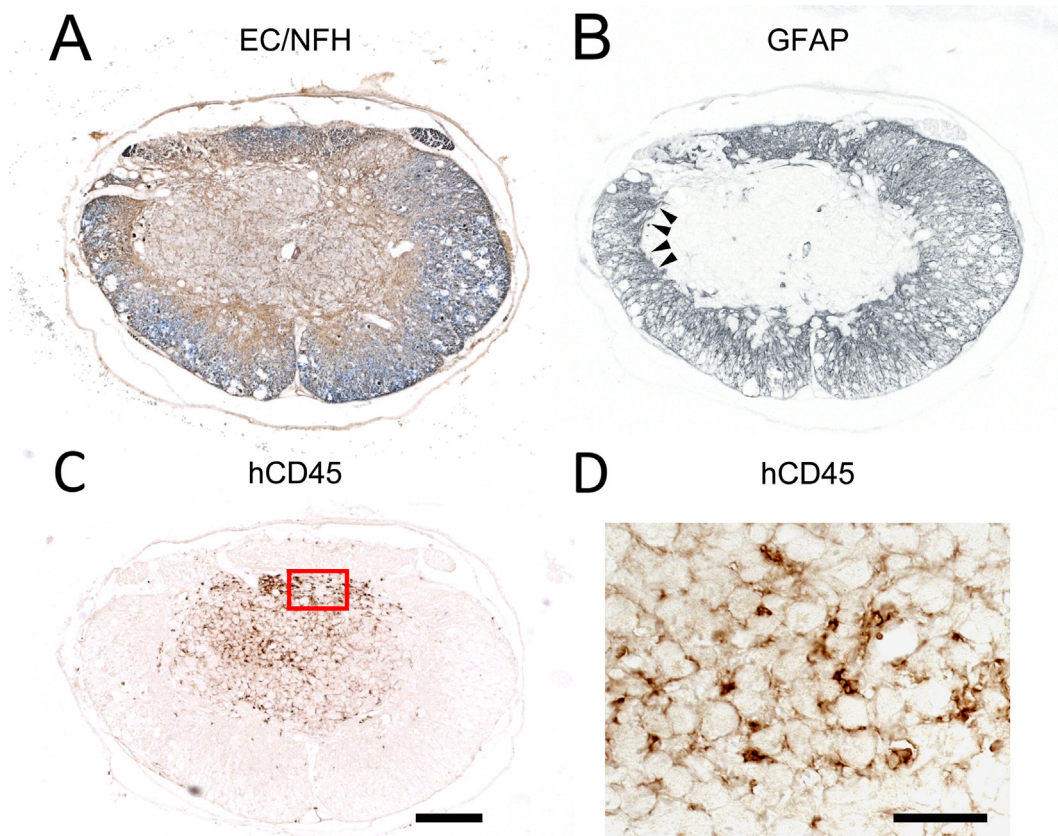


Fig. 4. Immunohistochemical staining in hNSG mouse spinal cord 28 dpi. (A) Eriochrome cyanine (blue) and neurofilament immunolabeling (brown) of spared white and gray matter surrounding a central core lesion. (B) Extensive astrogliosis, as defined by a prominent GFAP⁺ glial scar, surrounds the lesion (arrowheads delineate glial scar border). (C,D) hCD45⁺ human immune cells populate the lesion epicenter. Adjacent sections were used for A–D. Box in C delineates the location of high-powered image in D. Scale bars = 250 μm for A–C, and 50 μm in D. (For interpretation of the references to color in this figure legend, the reader is referred to the web version of this article.)

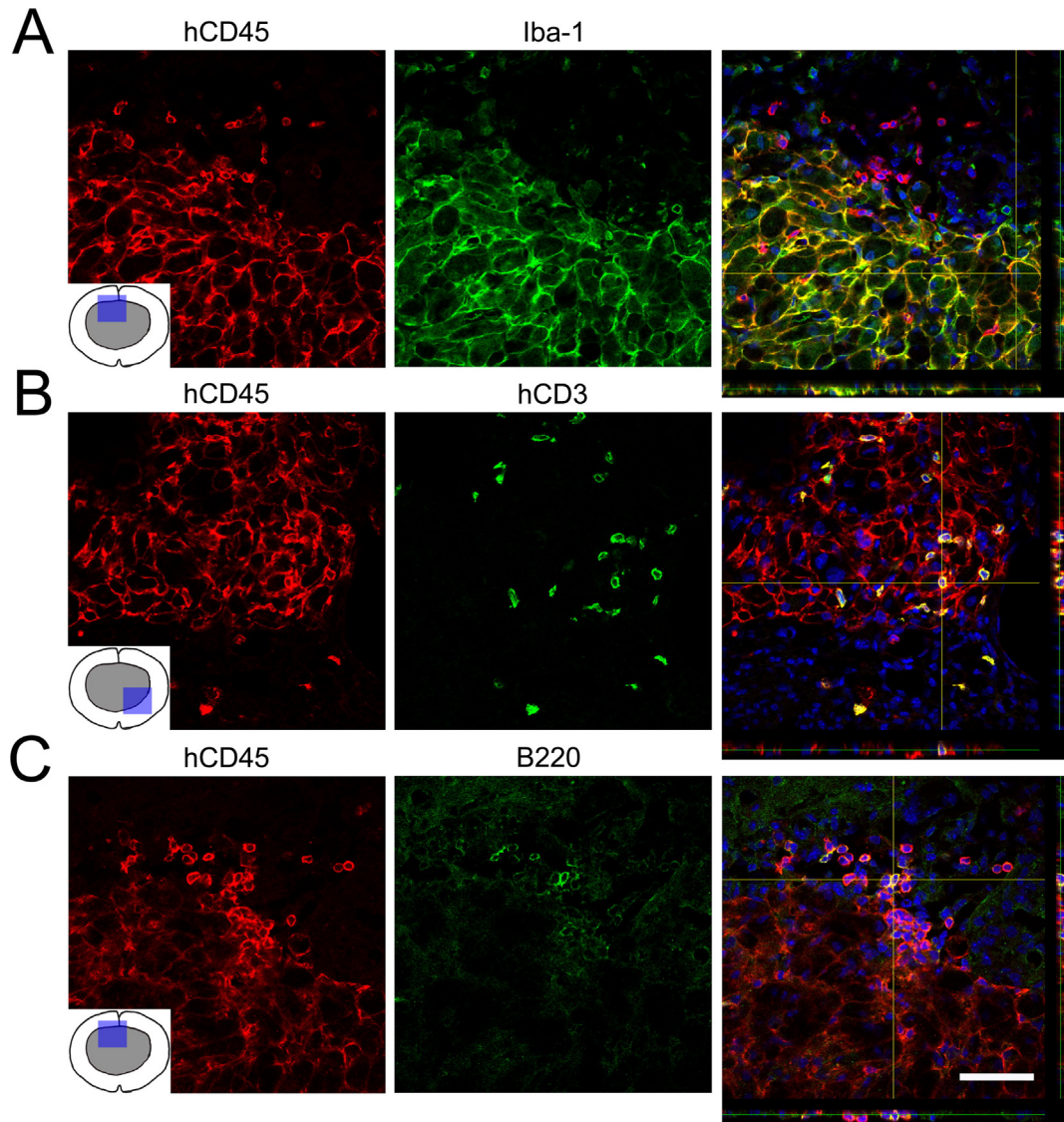


Fig. 5. Single plane and orthogonal views of fluorescent confocal Z stacks identifying specific types of human immune cells in the spinal cord of hNSG mice 28 dpi. (A) The lesion core was densely populated by large human macrophages (hCD45⁺/Iba-1⁺). (B) Human T cells (hCD45⁺/hCD3⁺) were dispersed throughout the lesion, frequently in small clusters. (C) Human B cells (hCD45⁺/B220⁺) also sparsely populated the injured spinal cord. Orthogonal views reveal immunofluorescent co-localization. Blue = DAPI nuclear stain. Scale bar = 50 μ m. (For interpretation of the references to color in this figure legend, the reader is referred to the web version of this article.)

general characteristics of revascularization and endogenous axon growth/sprouting, both of which occur naturally in rodent SCI models (Klapka and Müller, 2006; Loy et al., 2002).

Rostral to the lesion epicenter, CD31⁺ endothelia were found throughout gray and white matter, although profiles were more prevalent in gray matter (Fig. 7A). CD31⁺ blood vessels varied in size and were surrounded by a laminin-positive basement membrane. No human leukocytes (hCD45⁺ cells) were detected beyond zones of discernible pathology. In contrast, fewer CD31⁺ blood vessels were found at the epicenter but these were larger in diameter and were co-localized with a laminin-positive basal lamina or were interspersed between basal lamina “streamers” scattered throughout the lesion (Loy et al., 2002) (Fig. 7B). Most laminin streamers were not associated with CD31⁺ blood vessels. Instead, they co-localized with collagen and may serve as extracellular substrates for growing/spared axons. Indeed, neurofilament-positive axons appear to grow or sprout from spared white matter and enter the lesion core along GFAP⁺ astrocytes (Fig. 8A). However, within the core, most axons co-localized with collagen IV⁺ filament-like projections (Fig. 8B). The orthogonal plane of confocal images confirms the apposition of axons with collagen IV bundles,

interspersed between hCD45⁺ human immune cell clusters (arrows). The collagen IV response to SCI in hNSG mice is similar to that described in other rodent models (Klapka and Müller, 2006; Loy et al., 2002). These data indicate that human leukocytes either support or do not adversely affect normal endogenous repair mechanisms elicited by contusive SCI.

4. Discussion

Data in this report are the first to illustrate the feasibility of using humanized mice to test hypotheses related to neuro-immune interactions after traumatic spinal cord injury (SCI). Although mice have provided key insights to the cellular and molecular control of human immune system function, a recent study found that despite remarkable conservation of gene expression in mouse and human immune cells, divergent expression was noted for several hundred genes (Shay et al., 2013). These differences can be attributed to the heterogeneity of the human genome, as compared to inbred mice, but the fact remains that extrapolating immune data from mice into humans can be misleading (Mestas and Hughes, 2004).

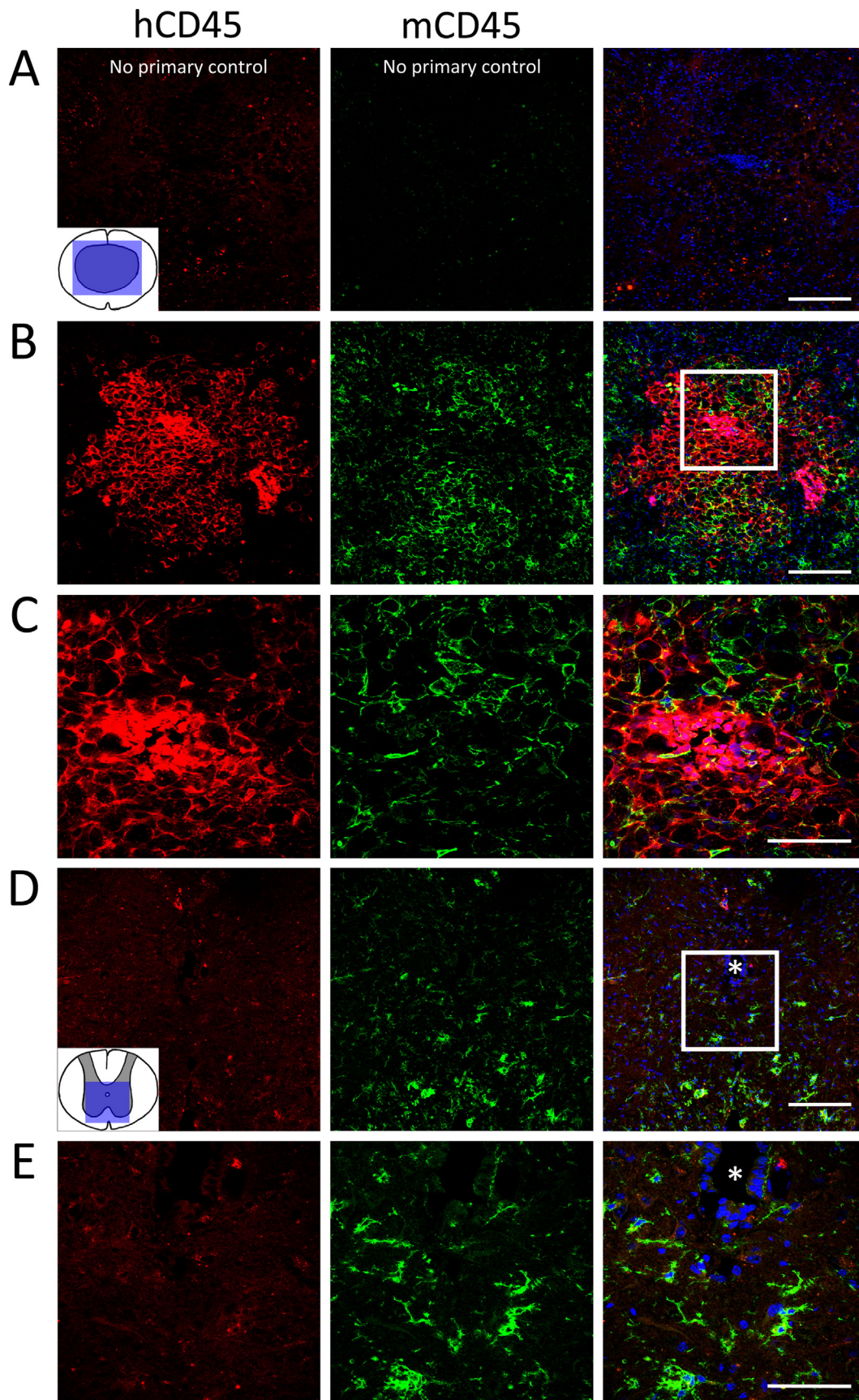


Fig. 6. Human CD45⁺ (hCD45) immune cells are restricted to the lesion epicenter and become co-localized with residual mouse CD45⁺ (mCD45) cells. (A) Specificity of labeling in epicenter sections was confirmed by omitting primary antibodies for mCD45 and hCD45. (B) Low-power confocal images reveal the spatial distribution of human (red) and mouse (green) leukocytes throughout the lesion epicenter at 28 dpi. (C) Higher-magnification of boxed region in (B). hCD45/mCD45⁺ double-labeling reveals that resident mouse CD45⁺ cells with microglia morphology dominate injured spinal cord in regions distal to the lesion epicenter (D,E). Scale bar = 150 μ m in A, B, & D; 100 μ m in C & E; blue = DAPI; *Denotes central canal in D & E. (For interpretation of the references to color in this figure legend, the reader is referred to the web version of this article.)

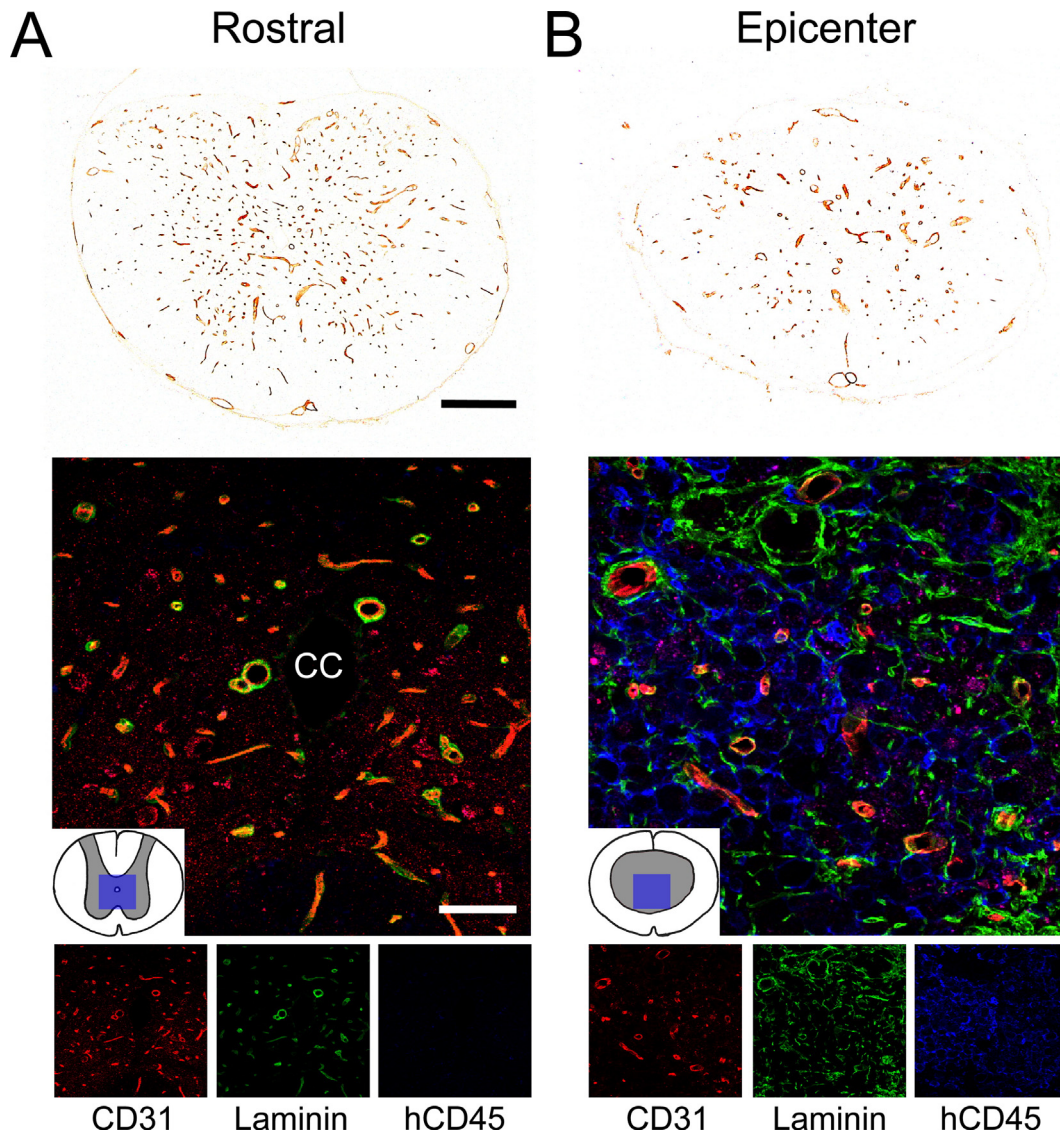


Fig. 7. Immunolabeling of spinal cord vasculature rostral to and at the lesion epicenter in an hNSG mouse 28 dpi. (A) Approximately 2 mm rostral to the lesion, laminin (green) was exclusively expressed around CD31⁺ blood vessels (red). No hCD45⁺ cells were observed in spinal cords outside of regions of pathology. (B) Spinal cord lesions contained extensive laminin expression (green) within and surrounding the lesion. CD31 immunolabeled vasculature (red) could be identified within the lesion core, co-labeled with laminin and dispersed among hCD45 positive human immune cells (blue). CC = central canal. Scale bar = 250 μ m for low powered CD31-DAB developed images; scale bar = 50 μ m for combined fluorescent images. Images in A and B were obtained from the same hNSG mouse. (For interpretation of the references to color in this figure legend, the reader is referred to the web version of this article.)

In humanized NSG (hNSG) mice, the full complement of human immune cells is produced. This makes it feasible to study immune cell phenotype and function *in vivo* in the context of dynamic pathological processes of relevance to SCI including the continuum of post-injury cell repair/cell death, cell transplantation, pharmacologic intervention, systemic infection, post-injury hematopoiesis, etc. Since most labs can easily incorporate humanized mice into their existing research infrastructure (e.g., injury models, core facilities and suites associated with surgery, behavior or housing), these mice can be used to overcome the complex logistics and ethical concerns that preclude translational SCI research in non-human primates (NHPs) and humans. Moreover, hNSG mice are significantly cheaper and infinitely easier to maintain and care for post-SCI than NHPs.

Our data indicate that when human hematopoietic stem cells are injected into young immune-deficient NSG mice, they differentiate into human immune cells that populate the blood and peripheral lymphoid organs. Importantly, engraftment occurs without eliciting graft-vs-host disease. Prior to SCI, all uninjured hNSG mice were healthy, i.e., none exhibited weight loss, porphyrin accumulation, vocalizations,

lethargy or behavioral impairment. Moreover, SCI did not prime a destructive systemic xenogeneic immune response. Indeed, all data obtained using humanized mice were indistinguishable from data that our lab and others have generated using other mouse strains (Basso et al., 2006; Kigerl et al., 2006; Luchetti et al., 2010; Sroga et al., 2003). Importantly, the pattern of human immune cell infiltration into the injured spinal cord of hNSG mice closely resembles what has been described in injured human spinal cords (Fleming et al., 2006; Chang, 2007). Also, the pattern of microglia and monocyte-derived macrophage distribution within the lesion core and surrounding spared tissues is stereotypical – resident microglia dominate the penumbra and spared tissue while most phagocytic cells in the lesion core derive from infiltrating monocyte-derived macrophages (see Popovich and Hickey, 2001; Mawhinney et al., 2012, and Fig. 6).

4.1. Potential limitations of the humanized mouse model

Despite the significant promise of this model, there are limitations that must be considered. Achieving optimal engraftment and differentiation of

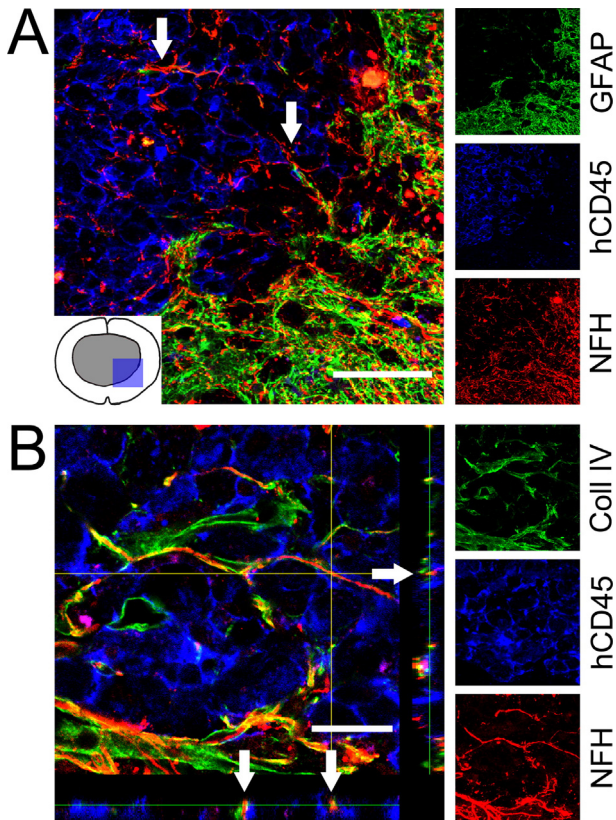


Fig. 8. Identifying sprouting and spared axons within the lesion of hNSG mice 28 dpi. (A) An astrocytic glial scar (GFAP⁺, green) surrounds a lesion core occupied by human immune cells (hCD45⁺, blue). Neurofilament-labeled axons (red) were predominantly located within the surrounding spared matter and glial scar, although some axons transverse the boundary of the glial scar and are present within the lesion (arrows). (B) Axons (red) within the lesion core project along deposits of the injury-induced extracellular matrix molecule collagen IV (green). Single plane orthogonal view highlights the intimate spatial relationship of axons, collagen IV, and human immune cells within the lesion (arrows). Scale bars = 80 μm in A and 25 μm in B. (For interpretation of the references to color in this figure legend, the reader is referred to the web version of this article.)

human hematopoietic stem cells requires that mice be exposed to myeloablative irradiation. Irradiation can cause systemic and neural pathology leading to muscle wasting, infection and in severe cases, death (Li et al., 2001, 2004; Qiu et al., 2010). We have shown that the CNS effects can be minimized or overcome completely using split-dose and low-dose irradiation protocols (Donnelly et al., 2011). Others have shown that systemic delivery of busulfan, an anti-neoplastic alkylating agent, can promote efficient chimerism without also adversely affecting the brain or spinal cord (Kierdorf et al., 2013). The newer, “next-generation” humanized mouse models could bypass the need for myeloablation altogether. Mouse hosts with viable mutations in the *Kit* oncogene lack c-Kit receptors and therefore cannot respond to stem cell factor, a requirement for endogenous hematopoiesis. By perturbing endogenous c-Kit-dependent signaling, engraftment of donor HSCs is favored. A recent report describes the stable and efficient engraftment of human HSCs injected into NSG/c-kit mutant hybrid mice (McIntosh et al., 2015). Currently, we cannot exclude the possibility that impaired functional recovery after SCI in hNSG mice relative to SCI non-irradiated NSG control mice is the result of adverse systemic or CNS effects caused by irradiation. However, previous data from our lab and others indicate that it is the phenotype and function of infiltrating leukocytes, not the irradiation protocol, that determines lesion pathology and functional recovery after SCI (Donnelly et al., 2011; Evans et al., 2014; Mawhinney et al., 2012; Shechter et al., 2009).

Given that spinal cord histopathology observed in SCI hNSG mice mimics what has been described in other mouse strains after SCI, one could conclude that human cells are irrelevant and that the anatomical

and functional changes are influenced only by residual mouse immune cells. This is unlikely for a few at least two reasons. First, NSG mice do not develop T or B lymphocytes (or NK cells) (Shultz et al., 2012). Thus, even though mouse lymphocytes have been shown to adversely affect spontaneous recovery in other mouse strains after SCI (Ankeny et al., 2009; Jones et al., 2002, 2005; Luchetti et al., 2010; Potas et al., 2006), they do not contribute in NSG mice. Second, even though endogenous neutrophils, monocytes and tissue macrophages, including CNS microglia, persist in NSG mice, the NOD genetic background contains alleles that render these cells dysfunctional (Shultz et al., 1995). Accordingly, human immune cells are likely to have the most significant functional impact in NSG humanized mice. In addition to the limitations listed above, it is possible that because human monocytes, macrophages and natural killer (NK) cells express cytokine receptors that do not cross-react with all mouse cytokines, optimal human innate immune cell development is impaired in humanized mice (Gille et al., 2012). However, a similar deficiency would be expected for T and B lymphocytes but these cells do develop in NSG mice.

Many factors can influence the reconstitution of human immune cells in humanized mice (e.g., source of HSCs, dose/route of cell injection, age or strain of the recipient). In our hands, the development of human myeloid cells and lymphocytes proceeds efficiently. At 10 weeks post-engraftment, ~8% of peripheral blood leukocytes are hCD45⁺. This reconstitution efficiency is consistent with reports from other laboratories (Lepus et al., 2009; Tanaka et al., 2012). Although this is a seemingly low percentage of all circulating cells, this underestimates the absolute numbers of human immune cells that exist in generative lymphoid tissues including bone marrow and spleen. Also, the ratio of human:mouse cells continues to increase as the mouse grows; by 17 weeks post-engraftment, ~60% of circulating leukocytes were hCD45⁺ and of these, ~25% were human monocytes. This is consistent with the proportion of monocytes found in other laboratories using humanized mice that were genetically engineered to express cytokines needed for human innate immune cell development (Rongvaux et al., 2014). Based on data in this manuscript, it is clear that a robust human immune cell repopulation occurs throughout the body and that in response to SCI, a robust cellular human inflammatory response of appropriate onset, magnitude and duration occurs at the injury site.

5. Conclusions

Since immune cells significantly affect neuron survival and axon growth and also are required to defend the body against infection, it is of paramount importance that the pathophysiological significance of SCI-induced changes in immune system function be determined. Humanized mouse models are ideally positioned to complement standard rodent models, and these mice will have a unique value within the SCI research community. Humanized mice allow for the direct study of human inflammation and immune function in vivo, with techniques that are currently impractical in human SCI patients. While humanized mice require a degree of specialized knowledge and resources, they are considerably less expensive and easier to work with than other large animal models (i.e. non-human primates). Such a platform may allow for the investigation of promising cell transplantation strategies, human specific immune modulatory therapies, and changes in immune function after SCI. Findings from such studies may aid in the discovery and translation of potential treatments with a goal for improving the quality of life for individuals with SCI.

Acknowledgments

This study was supported in part by NIH R01NS072304 (PGP), NINDS Core Grant (P30NS045758), the Ray W. Poppleton Endowment (PGP), and NCI P01CA100730 (SN). Funding agencies were not involved in the study design, collection and interpretation of data, or preparation of the manuscript.

Historical BMS data reprinted with permission from *Journal of Neurotrauma*, May 2006, Volume 23, Issue 5, pp. 635–659, published by Mary Ann Liebert Inc., New Rochelle, NY. Historical lesion volume data reprinted with permission from *Journal of Comparative Neurology*, February 2006, Volume 494, Issue 4, pp. 578–594, published by John Wiley & Sons Inc., Hoboken, NJ.

Images presented in this report were collected using instruments and services at the Campus Microscopy and Imaging Facility, The Ohio State University.

References

- Ankeny, D.P., Guan, Z., Popovich, P.G., 2009. B cells produce pathogenic antibodies and impair recovery after spinal cord injury in mice. *J. Clin. Invest.* 119, 2990–2999. <http://dx.doi.org/10.1172/JCI39780>.
- Anthony, D.C., Couch, Y., 2014. The systemic response to CNS injury. *Exp. Neurol.* 258, 105–111. <http://dx.doi.org/10.1016/j.expneurol.2014.03.013>.
- Auffray, C., Sieweke, M.H., Geissmann, F., 2009. Blood monocytes: development, heterogeneity, and relationship with dendritic cells. *Annu. Rev. Immunol.* 27, 669–692. <http://dx.doi.org/10.1146/annurev.immunol.021908.132557>.
- Basso, D.M., Fisher, L.C., Anderson, A.J., Jakeman, L.B., McTigue, D.M., Popovich, P.G., 2006. Basso Mouse Scale for locomotion detects differences in recovery after spinal cord injury in five common mouse strains. *J. Neurotrauma* 23, 635–659. <http://dx.doi.org/10.1089/neu.2006.23.635>.
- Blomster, L.V., Brennan, F.H., Lao, H.W., Harle, D.W., Harvey, A.R., Ruitenberg, M.J., 2013. Mobilisation of the splenic monocyte reservoir and peripheral CX3CR1 deficiency adversely affects recovery from spinal cord injury. *Exp. Neurol.* 247, 226–240. <http://dx.doi.org/10.1016/j.expneurol.2013.05.002>.
- Brehm, M.A., Cuthbert, A., Yang, C., Miller, D.M., Dilorio, P., Laning, J., Burzenski, L., Gott, B., Foreman, O., Kavirayani, A., Herlihy, M., Rossini, A.A., Shultz, L.D., Greiner, D.L., 2010. Parameters for establishing humanized mouse models to study human immunity: analysis of human hematopoietic stem cell engraftment in three immunodeficient strains of mice bearing the IL2rynull mutation. *Clin. Immunol.* 135, 84–98. <http://dx.doi.org/10.1016/j.clim.2009.12.008>.
- Campbell, S.J., Perry, V.H., Pitossi, F.J., Butchart, A.G., Chertoff, M., Waters, S., Dempster, R., Anthony, D.C., 2005. Central nervous system injury triggers hepatic CC and CXC chemokine expression that is associated with leukocyte mobilization and recruitment to both the central nervous system and the liver. *Am. J. Pathol.* 166, 1487–1497. [http://dx.doi.org/10.1016/S0002-9440\(10\)62365-6](http://dx.doi.org/10.1016/S0002-9440(10)62365-6).
- Campbell, S.J., Zahid, I., Losey, P., Law, S., Jiang, Y., Bilgen, M., van Rooijen, N., Morsali, D., Davis, A.E.M., Anthony, D.C., 2008. Liver Kupffer cells control the magnitude of the inflammatory response in the injured brain and spinal cord. *Neuropharmacology* 55, 780–787. <http://dx.doi.org/10.1016/j.neuropharm.2008.06.074>.
- Chang, H.T., 2007. Subacute human spinal cord contusion: few lymphocytes and many macrophages. *Spinal Cord* 45, 174–182. <http://dx.doi.org/10.1038/sj.sc.3101910>.
- Coughlan, A.M., Freeley, S.J., Robson, M.G., 2012. Humanised mice have functional human neutrophils. *J. Immunol. Methods* 385, 96–104. <http://dx.doi.org/10.1016/j.jim.2012.08.005>.
- Cros, J., Cagnard, N., Woollard, K., Patey, N., Zhang, S.Y., Senechal, B., Puel, A., Biswas, S.K., Moshous, D., Picard, C., Jais, J.P., D'Cruz, D., Casanova, J.L., Trouillet, C., Geissmann, F., 2010. Human CD14dim monocytes patrol and sense nucleic acids and viruses via TLR7 and TLR8 receptors. *Immunity* 33, 375–386. <http://dx.doi.org/10.1016/j.immuni.2010.08.012>.
- Donnelly, D.J., Longbrake, E.E., Shawler, T.M., Kigerl, K.A., Lai, W., Tovar, C.A., Ransohoff, R.M., Popovich, P.G., 2011. Deficient CX3CR1 signaling promotes recovery after mouse spinal cord injury by limiting the recruitment and activation of Ly6C^{hi}/iNOS⁺ macrophages. *J. Neurosci.* 31, 9910–9922. <http://dx.doi.org/10.1523/JNEUROSCI.2114-11.2011>.
- Evans, T.A., Barkauskas, D.S., Myers, J.T., Hare, E.G., You, J.Q., Ransohoff, R.M., Huang, A.Y., Silver, J., 2014. High-resolution intravital imaging reveals that blood-derived macrophages but not resident microglia facilitate secondary axonal dieback in traumatic spinal cord injury. *Exp. Neurol.* 254, 109–120. <http://dx.doi.org/10.1016/j.expneurol.2014.01.013>.
- Fleming, J.C., Norenberg, M.D., Ramsay, D.A., Dekaban, G.A., Marcillo, A.E., Saenz, A.D., Pasquale-Styles, M., Dietrich, W.D., Weaver, L.C., 2006. The cellular inflammatory response in human spinal cords after injury. *Brain* 129, 3249–3269. <http://dx.doi.org/10.1093/brain/awl296>.
- Fleming, J.C., Bailey, C.S., Hundt, H., Gurr, K.R., Bailey, S.I., Cepinskas, G., Lawendy, A.R., Badhwar, A., 2012. Remote inflammatory response in liver is dependent on the segmental level of spinal cord injury. *J. Trauma Acute Care Surg.* 72, 1194–1201. <http://dx.doi.org/10.1097/TA.0b013e31824d68bd>.
- Furlan, J.C., Krassioukov, A.V., Fehlings, M.G., 2006. Hematologic abnormalities within the first week after acute isolated traumatic cervical spinal cord injury: a case-control cohort study. *Spine (Phila Pa 1976)* 31, 2674–2683. <http://dx.doi.org/10.1097/01.brs.0000244569.91204.01>.
- Giassi, L.J., Pearson, T., Shultz, L.D., Laning, J., Biber, K., Kraus, M., Woda, B.A., Schmidt, M.R., Woodland, R.T., Rossini, A.A., Greiner, D.L., 2008. Expanded CD34⁺ human umbilical cord blood cells generate multiple lymphohematopoietic lineages in NOD-scid IL2rgamma(null) mice. *Exp. Biol. Med.* (Maywood) 233, 997–1012. <http://dx.doi.org/10.3181/0802-RM-70>.
- Gille, C., Orlikowsky, T.W., Spring, B., Hartwig, U.F., Wilhelm, A., Wirth, A., Goecke, B., Handgretinger, R., Poets, C.F., André, M.C., 2012. Monocytes derived from humanized neonatal NOD/SCID/IL2Ry null mice are phenotypically immature and exhibit functional impairments. *Hum. Immunol.* 73, 346–354. <http://dx.doi.org/10.1016/j.humimm.2012.01.006>.
- Huizinga, T.W., Roos, D., von dem Borne, A.E., 1990. Neutrophil Fc-gamma receptors: a two-way bridge in the immune system. *Blood* 75, 1211–1214.
- Inman, D., Guth, L., Steward, O., 2002. Genetic influences on secondary degeneration and wound healing following spinal cord injury in various strains of mice. *J. Comp. Neurol.* 451, 225–235. <http://dx.doi.org/10.1002/cne.10340>.
- Ishikawa, F., Yasukawa, M., Lyons, B., Yoshida, S., Miyamoto, T., Yoshimoto, G., Watanabe, T., Akashi, K., Shultz, L.D., Harada, M., 2005. Development of functional human blood and immune systems in NOD/SCID/IL2 receptor gamma chain^{mut} mice. *Blood* 106, 1565–1573. <http://dx.doi.org/10.1182/blood-2005-02-0516>.
- Jones, T.B., Basso, D.M., Sodhi, A., Pan, J.Z., Hart, R.P., MacCallum, R.C., Lee, S., Whitacre, C.C., Popovich, P.G., 2690–700, 2002. Pathological CNS autoimmune disease triggered by traumatic spinal cord injury: implications for autoimmune vaccine therapy. *J. Neurosci.* 22 (doi:20026267).
- Jones, T.B., Hart, R.P., Popovich, P.G., 2005. Molecular control of physiological and pathological T-cell recruitment after mouse spinal cord injury. *J. Neurosci.* 25, 6576–6583. <http://dx.doi.org/10.1523/JNEUROSCI.0305-05.2005>.
- Kierdorf, K., Katzmarzki, N., Haas, C.A., Prinz, M., 2013. Bone marrow cell recruitment to the brain in the absence of irradiation or parabiosis bias. *PLoS One* 8, 1–10. <http://dx.doi.org/10.1371/journal.pone.0058544>.
- Kigerl, K.A., McLaughly, V.M., Popovich, P.G., 2006. Comparative analysis of lesion development and intraspinal inflammation in four strains of mice following spinal contusion injury. *J. Comp. Neurol.* 494, 578–594. <http://dx.doi.org/10.1002/cne.20827>.
- Kigerl, K.A., Gensel, J.C., Ankeny, D.P., Alexander, J.K., Donnelly, D.J., Popovich, P.G., 2009. Identification of two distinct macrophage subsets with divergent effects causing either neurotoxicity or regeneration in the injured mouse spinal cord. *J. Neurosci.* 29, 13435–13444. <http://dx.doi.org/10.1523/JNEUROSCI.3257-09.2009>.
- Klapka, N., Müller, H.W., 2006. Collagen matrix in spinal cord injury. *J. Neurotrauma* 23, 422–435. <http://dx.doi.org/10.1089/neu.2006.23.422>.
- Lander, E.S., Linton, L.M., Birren, B., Nusbaum, C., Zody, M.C., Baldwin, J., Devon, K., Dewar, K., Doyle, M., FitzHugh, W., Funke, R., Gage, D., Harris, K., Heaford, A., Howland, J., Kann, L., Lehoczky, J., LeVine, R., McEwan, P., McKernan, K., Meldrum, J., Mesirov, J.P., Miranda, C., Morris, W., Naylor, J., Raymond, C., Rosetti, M., Santos, R., Sheridan, A., Sougnez, C., Stange-Thomann, N., Stojanovic, N., Subramanian, A., Wyman, D., Rogers, J., Sulston, J., Ainscough, R., Beck, S., Bentley, D., Burton, J., Clee, C., Carter, N., Coulson, A., Deadman, R., Deloukas, P., Dunham, A., Dunham, I., Durbin, R., French, L., Grafham, D., Gregory, S., Hubbard, T., Humphray, S., Hunt, A., Jones, M., Lloyd, C., McMurray, A., Matthews, L., Mercer, S., Milne, S., Mullikin, J.C., Mungall, A., Plumb, R., Ross, M., Showlkeen, R., Sims, S., Waterston, R.H., Wilson, R.K., Hillier, L.W., McPherson, J.D., Marra, M.A., Mardis, E.R., Fulton, L.A., Chinwalla, A.T., Pepin, K.H., Gish, W.R., Chissoe, S.L., Wendl, M.C., Delehaunty, K.D., Miner, T.L., Delehaunty, A., Kramer, J.B., Cook, L.L., Fulton, R.S., Johnson, D.L., Minx, P.J., Clifton, S.W., Hawkins, T., Branscomb, E., Predki, P., Richardson, P., Wenning, S., Slezak, T., Doggett, N., Cheng, J.F., Olsen, A., Lucas, S., Elkin, C., Uberbacher, E., Frazier, M., Gibbs, R.A., Muzny, D.M., Scherer, S.E., Bouck, J.B., Sodergren, E.J., Worley, K.C., Rives, C.M., Gorrell, J.H., Metzker, M.L., Naylor, S.L., Kucherlapati, R.S., Nelson, D.L., Weinstock, G.M., Sakaki, Y., Fujiiyama, A., Hattori, M., Yada, T., Toyoda, A., Itoh, T., Kawagoe, C., Watanabe, H., Totoki, Y., Taylor, T., Weissbach, J., Heilig, R., Saurin, W., Artiguenave, F., Brottier, P., Bruls, T., Pelletier, E., Robert, C., Wincker, P., Smith, D.R., Doucette-Stamm, L., Rubenfield, M., Weinstock, K., Lee, H.M., Dubois, J., Rosenthal, A., Platzer, M., Nyakatura, G., Taudien, S., Rump, A., Yang, H., Yu, J., Wang, J., Huang, G., Gu, J., Hood, L., Rowen, L., Madan, A., Qin, S., Davis, R.W., Federspiel, N.A., Abola, A.P., Proctor, M.J., Myers, R.M., Schmutz, J., Dickinson, M., Grimwood, J., Cox, D.R., Olson, M.V., Kaul, R., Raymond, C., Shimizu, N., Kawasaki, K., Minoshima, S., Evans, G.A., Athanasiou, M., Schultz, R., Roe, B.A., Chen, F., Pan, H., Ramser, J., Lehrach, H., Reinhardt, R., McCombie, W.R., de la Bastide, M., Dedhia, N., Böcker, H., Hornischer, K., Nordsiek, G., Agarwala, R., Aravind, L., Bailey, J.A., Bateman, A., Batzoglou, S., Birney, E., Bork, P., Brown, D.G., Burge, C.B., Cerutti, L., Chen, H.C., Church, D., Clamp, M., Copley, R.R., Doerks, T., Eddy, S.R., Eichler, E.E., Furey, T.S., Galagan, J., Gilbert, J.G., Harmon, C., Hayashizaki, Y., Haussler, D., Hermjakob, H., Hokamp, K., Jang, W., Johnson, L.S., Jones, T.A., Kasif, S., Kasprzyk, A., Kennedy, S., Kent, W.J., Kitts, P., Koonin, E.V., Korf, I., Kulp, D., Lancet, D., Lowe, T.M., McLysaght, A., Mikkelsen, T., Moran, J.V., Mulder, N., Pollara, V.J., Ponting, C.P., Schuler, G., Schultz, J., Slater, G., Smit, A.F., Stupka, E., Szustakowski, J., Thierry-Mieg, D., Thierry-Mieg, J., Wagner, L., Wallis, J., Wheeler, R., Williams, A., Wolf, Y.I., Wolfe, K.H., Yang, S.P., Ye, R.F., Collins, F., Guyer, M.S., Peterson, J., Felsenfeld, A., Wetterstrand, K.A., Patrino, A., Morgan, M.J., de Jong, P., Catanese, J.J., Osoegawa, K., Shizuya, H., Choi, S., Chen, Y.J., 2001. Initial sequencing and analysis of the human genome. *Nature* 409, 860–921. <http://dx.doi.org/10.1038/35057062>.
- Lanier, L.L., Le, A.M., Civin, C.I., Loken, M.R., Phillips, J.H., 1986. The relationship of CD16 (Leu-11) and Leu-19 (NKH-1) antigen expression on human peripheral blood NK cells and cytotoxic T lymphocytes. *J. Immunol.* 136, 4480–4486.
- Lepus, C.M., Gibson, T.F., Gerber, S.A., Kawikova, I., Szczepanik, M., Hossain, J., Ablamunits, V., Kirkiles-Smith, N., Herold, K.C., Donis, R.O., Bothwell, A.L., Pober, J.S., Harding, M.J., 2009. Comparison of human fetal liver, umbilical cord blood, and adult blood hematopoietic stem cell engraftment in NOD-scid/yc^{-/-}, Balb/c-Rag1^{-/-}yc^{-/-}, and C.B-17-scid/bg immunodeficient mice. *Hum. Immunol.* 70, 790–802. <http://dx.doi.org/10.1016/j.humimm.2009.06.005>.
- Li, Y.Q., Ballinger, J.R., Nordal, R.A., Su, Z.F., Wong, C.S., 2001. Hypoxia in radiation-induced blood–spinal cord barrier breakdown. *Cancer Res.* 61, 3348–3354.
- Li, Y.-Q., Chen, P., Jain, V., Reilly, R.M., Wong, C.S., 2004. Early radiation-induced endothelial cell loss and blood–spinal cord barrier breakdown in the rat spinal cord. *Radiat. Res.* 161, 143–152. <http://dx.doi.org/10.1667/RR3117>.
- Loy, D.N., Crawford, C.H., Darnall, J.B., Burke, D.A., Onifer, S.M., Whittemper, S.R., 2002. Temporal progression of angiogenesis and basal lamina deposition after contusive

- spinal cord injury in the adult rat. *J. Comp. Neurol.* 445, 308–324. <http://dx.doi.org/10.1002/cne.10168>.
- Luchetti, S., Beck, K.D., Galvan, M.D., Silva, R., Cummings, B.J., Anderson, A.J., 2010. Comparison of immunopathology and locomotor recovery in C57BL/6, BUB/BnJ, and NOD-SCID mice after contusion spinal cord injury. *J. Neurotrauma* 27, 411–421. <http://dx.doi.org/10.1089/neu.2009.0930>.
- Mawhinney, L.A., Thawer, S.G., Lu, W.-Y., Rooijen, N., Van, Weaver, L.C., Brown, A., Dekaban, G.A., 2012. Differential detection and distribution of microglial and hematogenous macrophage populations in the injured spinal cord of lys-EGFP-ki transgenic mice. *J. Neuropathol. Exp. Neurol.* 71, 180–197. <http://dx.doi.org/10.1097/NEN.0b013e3182479b41>.
- McIntosh, B.E., Brown, M.E., Duffin, B.M., Maufort, J.P., Vereide, D.T., Slukvin, I.I., Thomson, J.A., 2015. Nonirradiated NOD, B6.SCID IL2 $\gamma^{-/-}$ Kit^{W41/W41} (NBSGW) mice support multilineage engraftment of human hematopoietic cells. *Stem Cell Rep.* 4, 171–180. <http://dx.doi.org/10.1016/j.stemcr.2014.12.005>.
- Mestas, J., Hughes, C.C.W., 2004. Of mice and not men: differences between mouse and human immunology. *J. Immunol.* 172, 2731–2738. <http://dx.doi.org/10.4049/jimmunol.172.5.2731>.
- Popovich, P.G., Hickey, W.F., 2001. Bone marrow chimeric rats reveal the unique distribution of resident and recruited macrophages in the contused rat spinal cord. *J. Neuropathol. Exp. Neurol.* 60, 676–685.
- Potas, J.R., Zheng, Y., Moussa, C., Venn, M., Gorrie, C.A., Deng, C., Waite, P.M.E., 2006. Augmented locomotor recovery after spinal cord injury in the athymic nude rat. *J. Neurotrauma* 23, 660–673. <http://dx.doi.org/10.1089/neu.2006.23.660>.
- Qiu, W., Leibowitz, B., Zhang, L., Yu, J., 2010. Growth factors protect intestinal stem cells from radiation-induced apoptosis by suppressing PUMA through the PI3K/AKT/p53 axis. *Oncogene* 29, 1622–1632. <http://dx.doi.org/10.1158/1538-7445.AM10-3198>.
- Rajesh, D., Zhou, Y., Jankowska-Gan, E., Roenneburg, D.A., Dart, M.L., Torrealba, J., Burlingham, W.J., 2010. Th1 and Th17 immunocompetence in humanized NOD/SCID/IL2 γ^{null} mice. *Hum. Immunol.* 71, 551–559. <http://dx.doi.org/10.1016/j.humimm.2010.02.019>.
- Riegger, T., Conrad, S., Schluesener, H.J., Kaps, H.P., Badke, A., Baron, C., Gerstein, J., Dietz, K., Abdizahdeh, M., Schwab, J.M., 2009. Immune depression syndrome following human spinal cord injury (SCI): a pilot study. *Neuroscience* 158, 1194–1199. <http://dx.doi.org/10.1016/j.neuroscience.2008.08.021>.
- Rongvaux, A., Willinger, T., Martinek, J., Strowig, T., Gearty, S.V., Teichmann, L.L., Saito, Y., Marches, F., Halene, S., Palucka, K., Manz, M.G., Flavell, R.A., 2014. Development and function of human innate immune cells in a humanized mouse model. *Nat. Biotechnol.* 32, 364–372. <http://dx.doi.org/10.1038/nbt.2858>.
- Sauerbeck, A.D., Laws, J.L., Bandaru, V.V.R., Popovich, P.G., Haughey, N.J., McTigue, D.M., 2015. Spinal cord injury causes chronic liver pathology in rats. *J. Neurotrauma* 32, 159–169. <http://dx.doi.org/10.1089/neu.2014.3497>.
- Schwab, J.M., Zhang, Y., Kopp, M.A., Brommer, B., Popovich, P.G., 2014. The paradox of chronic neuroinflammation, systemic immune suppression, autoimmunity after traumatic chronic spinal cord injury. *Exp. Neurol.* 258, 121–129. <http://dx.doi.org/10.1016/j.expneurol.2014.04.023>.
- Seok, J., Warren, H.S., Cuenca, A.G., Mindrinos, M.N., Baker, H.V., Xu, W., Richards, D.R., McDonald-Smith, G.P., Gao, H., Hennessy, L., Finnerty, C.C., López, C.M., Honari, S., Moore, E.E., Minei, J.P., Cuschieri, J., Bankey, P.E., Johnson, J.L., Sperry, J., Nathens, A.B., Billiar, T.R., West, M. a, Jeschke, M.G., Klein, M.B., Gamelli, R.L., Gibran, N.S., Brownstein, B.H., Miller-Graziano, C., Calvano, S.E., Mason, P.H., Cobb, J.P., Rahme, L.G., Lowry, S.F., Maier, R.V., Moldawer, L.L., Herndon, D.N., Davis, R.W., Xiao, W., Tompkins, R.G., 2013. Genomic responses in mouse models poorly mimic human inflammatory diseases. *Proc. Natl. Acad. Sci. U. S. A.* 110, 3507–3512. <http://dx.doi.org/10.1073/pnas.1222878110>.
- Shay, T., Jojic, V., Zuk, O., Rothamel, K., Puyraimond-Zemmour, D., Feng, T., Wakamatsu, E., Benoist, C., Koller, D., Regev, A., 2013. Conservation and divergence in the transcriptional programs of the human and mouse immune systems. *Proc. Natl. Acad. Sci. U. S. A.* 110, 2946–2951. <http://dx.doi.org/10.1073/pnas.1222738110>.
- Shechter, R., London, A., Varol, C., Raposo, C., Cusimano, M., Yovel, G., Rolls, A., Mack, M., Pluchino, S., Martino, G., Jung, S., Schwartz, M., 2009. Infiltrating blood-derived macrophages are vital cells playing an anti-inflammatory role in recovery from spinal cord injury in mice. *PLoS Med.* 6. <http://dx.doi.org/10.1371/journal.pmed.1000113>.
- Shultz, L.D., Schweitzer, P.a, Christianson, S.W., Gott, B., Schweitzer, I.B., Tennent, B., McKenna, S., Mobraaten, L., Rajan, T.V., Greiner, D.L., 1995. Multiple defects in innate and adaptive immunologic function in NOD/LtSz-scid mice. *J. Immunol.* 154, 180–191.
- Shultz, L.D., Lyons, B.L., Burzenski, L.M., Gott, B., Chen, X., Chaleff, S., Kotb, M., Gillies, S.D., King, M., Mangada, J., Greiner, D.L., Handgretinger, R., 2005. Human lymphoid and myeloid cell development in NOD/LtSz-scid IL2R gamma null mice engrafted with mobilized human hemopoietic stem cells. *J. Immunol.* 174, 6477–6489. <http://dx.doi.org/10.4049/jimmunol.174.10.6477>.
- Shultz, L.D., Ishikawa, F., Greiner, D.L., 2007. Humanized mice in translational biomedical research. *Nat. Rev. Immunol.* 7, 118–130. <http://dx.doi.org/10.1038/nri2017>.
- Shultz, L.D., Brehm, M., Garcia-Martinez, J.V., Greiner, D.L., 2012. Humanized mice for immune system investigation: progress, promise and challenges. *Nat. Rev. Immunol.* 12, 786–798. <http://dx.doi.org/10.1038/nri3311>.
- Sroga, J.M., Jones, T.B., Kigerl, K.A., McLaughly, V.M., Popovich, P.G., 2003. Rats and mice exhibit distinct inflammatory reactions after spinal cord injury. *J. Comp. Neurol.* 462, 223–240. <http://dx.doi.org/10.1002/cne.10736>.
- Tanaka, S., Saito, Y., Kunisawa, J., Kurashima, Y., Wake, T., Suzuki, N., Shultz, L.D., Kiyono, H., Ishikawa, F., 2012. Development of mature and functional human myeloid subsets in hematopoietic stem cell-engrafted NOD/SCID/IL2r KO mice. *J. Immunol.* 188, 6145–6155. <http://dx.doi.org/10.4049/jimmunol.1103660>.
- Urrea, X., Villamor, N., Amaro, S., Gómez-Choco, M., Obach, V., Oleaga, L., Planas, A.M., Chamorro, A., 2009. Monocyte subtypes predict clinical course and prognosis in human stroke. *J. Cereb. Blood Flow Metab.* 29, 994–1002. <http://dx.doi.org/10.1038/jcbfm.2009.25>.
- Waterston, R.H., Lindblad-Toh, K., Birney, E., Rogers, J., Abril, J.F., Agarwal, P., Agarwala, R., Ainscough, R., Alexandersson, M., An, P., Antonarakis, S.E., Attwood, J., Baertsch, R., Bailey, J., Barlow, K., Beck, S., Berry, E., Birren, B., Bloom, T., Bork, P., Botcherby, M., Bray, N., Brent, M.R., Brown, D.G., Brown, S.D., Bult, C., Burton, J., Butler, J., Campbell, R.D., Carninci, P., Cawley, S., Chiaromonte, F., Chinwalla, A.T., Church, D.M., Clamp, M., Clee, C., Collins, F.S., Cook, L.L., Copley, R.R., Coulson, A., Couronne, O., Cuff, J., Curwen, V., Cutts, T., Daly, M., David, R., Davies, J., Delehaunty, K.D., Deri, J., Dermitzakis, E.T., Dewey, C., Dickens, N.J., Diekhans, M., Dodge, S., Dubchak, I., Dunn, D.M., Eddy, S.R., Elnitski, L., Emes, R.D., Eswara, P., Eyraes, E., Felsenfeld, A., Fellwold, G.A., Flicek, P., Foley, K., Frankel, W.N., Fulton, L.A., Fulton, R.S., Furey, T.S., Gage, D., Gibbs, R.A., Glusman, G., Gnerre, S., Goldman, N., Goodstadt, L., Graffham, D., Graves, T.A., Green, E.D., Gregory, S., Guigó, R., Guyer, M., Hardison, R.C., Haussler, D., Hayashizaki, Y., Hillier, L.W., Hinrichs, A., Hlavina, W., Holzer, T., Hsu, F., Hua, A., Hubbard, T., Hunt, A., Jackson, I., Jaffe, D.B., Johnson, L.S., Jones, M., Jones, T.A., Joy, A., Kamal, M., Karlsson, E.K., Karolchik, D., Kasprzyk, A., Kawai, J., Keibler, E., Kells, C., Kent, W.J., Kirby, A., Kolbe, D.L., Korf, I., Kucherlapati, R.S., Kulbokas, E.J., Kulp, D., Landers, T., Leger, J.P., Leonard, S., Letunic, I., Levine, R., Li, J., Li, M., Lloyd, C., Lucas, S., Ma, B., Maglott, D.R., Mardis, E.R., Matthews, L., Mauceli, E., Mayer, J.H., McCarthy, M., McCombie, W.R., McLaren, S., McLay, K., McPherson, J.D., Meldrim, J., Meredith, B., Mesirov, J.P., Miller, W., Miner, T.L., Mongin, E., Montgomery, K.T., Morgan, M., Mott, R., Mullikin, J.C., Muzny, D.M., Nash, W.E., Nelson, J.O., Nhan, M.N., Nicol, R., Ning, Z., Nusbaum, C., O'Connor, M.J., Okazaki, Y., Oliver, K., Overton-Larty, E., Pachter, L., Parra, G., Pepin, K.H., Peterson, J., Pevzner, P., Plumb, R., Pohl, C.S., Poliakov, A., Ponce, T.C., Ponting, C.P., Potter, S., Quail, M., Reymond, A., Roe, B. a, Roskin, K.M., Rubin, E.M., Rust, A.G., Santos, R., Sapojnikov, V., Schultz, B., Schultz, J., Schwartz, M.S., Schwartz, S., Scott, C., Seaman, S., Searle, S., Sharpe, T., Sheridan, A., Showkeen, R., Sims, S., Singer, J.B., Slater, G., Smit, A., Smith, D.R., Spencer, B., Stabenau, A., Stange-Thomann, N., Sugnet, C., Suyama, M., Tesler, G., Thompson, J., Torrents, D., Trevaskis, E., Tromp, J., Ucla, C., Ureta-Vidal, A., Vinson, J.P., Von Niederhausern, A.C., Wade, C.M., Wall, M., Weber, R.J., Weiss, R.B., Wendl, M.C., West, A.P., Wetterstrand, K., Wheeler, R., Whelan, S., Wierzbowski, J., Willey, D., Williams, S., Wilson, R.K., Winter, E., Worley, K.C., Wyman, D., Yang, S., Yang, S.-P., Zdobnov, E.M., Zody, M.C., Lander, E.S., 2002. Initial sequencing and comparative analysis of the mouse genome. *Nature* 420, 520–562. <http://dx.doi.org/10.1038/nature01262>.